Catal Lett (2009) 129:367–375
DOI 10.1007/s10562-008-9793-x

Enantioselective Epoxidation of Alkenes by *Jacobsen* Catalyst Anchored onto Aminopropyl-functionalised Laponite, MCM-41 and FSM-16

Pankaj Das · Ana Rosa Silva · Ana P. Carvalho · João Pires · Cristina Freire

Received: 17 January 2008 / Accepted: 20 November 2008 / Published online: 5 December 2008

Abstract The *Jacobsen* catalyst derivative, (*R*,*R*)-[Mn(3,5-dtButsalhd)]ClO_4–CAT 2, was immobilized through axial coordination of the metal center onto a Laponite, MCM-41 and FSM-16 functionalized with 3-aminopropyltriethoxysilane. The catalytic activity of the Mn-based materials was screened for the enantioselective epoxidation of three olefins: styrene, α-methylstyrene and 6-CN-2,2′-dimethychromene, using m-CPBA/NMO as oxidant, and the results were compared with the corresponding homogenous complex (CAT 2) and with the *Jacobsen*'s catalyst, (*R*,*R*)-[Mn(3,5-dtButsalhd)Cl]–CAT 1. The results indicate that under comparable condition, the Laponite-based materials show both, higher epoxide yield and enantiomeric excess (ee%) compared to MCM-41 and FSM-16-based materials. The best ee% value was obtained for the substrate 6-CN-2,2′-dimethylchromene (64%) which is very close to that obtained with CAT 2 (67%) in homogeneous phase; for the two regular mesoporous materials (MCM-41 and FSM-16) the catalytic results were more favorable for the FSM-16 samples.

Keywords Enantioselective epoxidation · Chiral Mn(III) *salen* complex · Laponite · MCM-41 · FSM-16 · Covalent anchoring

1 Introduction

Chiral manganese(III) *salen* complexes are highly efficient homogeneous catalysts in the asymmetric epoxidation of several un-functionalized alkenes [1–3]. Conversely, chiral epoxides are extremely useful building blocks in the synthesis of chiral compounds for the pharmaceutical as well as for agrochemical industries [1–3]. Therefore, chemical sustainability of this homogeneous catalyst has been attracting attention of researchers [4–6], since it can not be recycled. One of the solutions that has been extensively researched is the immobilization of the chiral manganese(III) *salen* complexes into/onto insoluble supports, which prevents the formation of inactive dimeric Mn(IV) (the main deactivation process in homogeneous phase) and allows for their recovery by simple filtration [4–6].

Initially organic polymers were extensively used to covalently anchor Mn(III) *salen* catalysts, but limited success was reported mainly due to the lack of stability of the supports under the epoxidazing conditions [7–12]. Due to their higher stability in reaction media, inorganic

---

Electronic supplementary material The online version of this article (doi:10.1007/s10562-008-9793-x) contains supplementary material, which is available to authorized users.

P. Das · A. R. Silva · C. Freire (✉)
REQUIMTE/Departamento de Química, Faculdade de Ciências, Universidade do Porto, Rua do Campo Alegre, 4169-007 Porto, Portugal
e-mail: acfreire@fc.up.pt

A. P. Carvalho · J. Pires
Departamento de Química e Bioquímica and CQB, Faculdade de Ciências, Universidade de Lisboa, Ed. C8, Campo Grande, 1749-016 Lisbon, Portugal

Present Address:
P. Das
Department of Chemistry, Dibrugarh University, Dibrugarh, Assam 786 004, India

Present Address:
A. R. Silva
Unilever R&D, Port Sunlight, Bebington, UK

materials started to be used, being the first reports on the Mn(III) *salen* encapsulation into zeolites [13–16]. With the development of ordered mesoporous materials, several reports were published on the covalent attachment of Mn(III) *salen* catalysts mainly on MCM-41 [17–26]. The covalent attachment through the ligand has generally led to reduce activity and enantioselectivity compared to the homogeneous counterparts [17–19], probably due to the structural/electronic modifications introduced in the *salen* ligand to allow for its covalent attachment [27].

Recently, the anchoring of [M (*salen*)] catalysts [M = transition cation] into mesoporous materials through axial coordination to the metal center have been published, with specific emphasis on the improved enantioselectivity in comparison to their homogeneous counterparts [20–26, 28–33]. Despite the efficiency of some of immobilization strategies, they usually involve multi-step procedures which often require time-consuming synthetic manipulations, thus limiting their application; therefore, the demand for simpler and effective procedures to prepare heterogenized Mn(III) *salen* catalysts is still a topic of major importance.

Clays have been used in the past to immobilize Mn(III) *salen* catalysts by ion exchange of interlayer cations [34–37], but, recently Laponite, which has regular crystallites of small size (in the range of the several nm) with reactive surface Si–OH group located at the edge of the clay sheets [38], was used to immobilize a non-chiral Mn(III) *salen* complex through encapsulation and edge modification [39].

The preparation of porous solids from layered silicates by the interlayer cross linking of the silicate layers by the reaction with alkyl trimethyl ammonium ions, was proposed in the 1990s [40–42]. The layered silicate used was kanemite and the resulting material, the FSM-16 solid, presented a regular structure with channel type mesopores [40–42]. Structurally, FSM-16 material has some similarity to the well known MCM-41 solid [43, 44] but, apparently, with higher structural stability [42].

In the sequence of our previous reports on the preparation and characterization of the *Jacobsen* catalyst (CAT 1) and its perchlorate derivative (CAT 2) anchored onto amino-functionalized Laponite, MCM-41 [45] and FSM-16 materials [46], herein we report their catalytic activity in the asymmetric epoxidation of three alkenes (styrene, α-Me-styrene and 6-CN-2,2′-dimethylchromene) by using *m*-CPBA/NMO as the oxygen source. Due to the different supports used (MCM-41 and FSM-16 are regular mesoporous silicas, while Laponite is also a mesoporous material but with mesoporosity resulting from interparticle aggregates), in this report we endeavor to prove the support effect and anchoring strategy on the asymmetric epoxidation outcome of the immobilized catalysts.

2 Experimental

2.1 Parent Materials, Solvents and Reagents

Laponite was obtained from Laporte Industries Ltd. and was used as received. Its structural formula, as indicated by the supplier, is $Na_{0.7}[(Si_8Mg_{5.5}Li_{0.3})O_{20}(OH)_4]$. The MCM-41 was synthesized according to procedures described in the literature [47]; from the results of powder XRD the peaks corresponding to d_{100}, d_{110} and d_{200} were at values of 3.78, 2.17 and 1.91 nm, respectively, within the range of published values [47]. The a_0 parameter of the prepared sample, considering a hexagonal symmetry, is 4.37 nm. The parent FSM-16, kindly supplied by Toyota Central R&D Labs, was used as received, and will be labeled as F1; considering the hexagonal symmetry, its a_0 parameter is 4.41 nm. More details on the structure of the solids are given in the Supporting Information (SI1): structures of Laponite, MCM-41 and FSM-16.

Tetraethoxysilane, cetyltrimethylammonium bromide, (*R*,*R*)-(−)-*N*,*N*′-Bis(3,5-di-*tert*-butylsalicylidene)-1,2-cyclohexanediaminomanganese(III) chloride (the *Jacobsen* catalyst, CAT1), silver perchlorate, 3-aminopropyltriethoxysilane (APTES), sodium etoxide solution (21%) in ethanol (NaOEt), styrene, α-methylstyrene (α-Me-styrene), 6-cyano-2,2-dimethylchromene (6-CN-chromene), chlorobenzene, benzaldehyde, styrene epoxide, *m*-chloroperoxybenzoic acid (*m*-CPBA) and 4-methylmorpholine *N*-oxide (NMO) were purchased from Aldrich. Aqueous ammonia and all the solvents used were purchased from Merck (*pro analysi*), except dichloromethane used in the catalytic experiments which was from Romil (HPLC grade).

2.2 Preparation of Materials

2.2.1 *Modification of Supporting Materials*

Anchoring of APTES onto Laponite, MCM-41 or FSM-16: laponite, MCM-41 and FSM-16 were functionalized with APTES by following a method described in the literature [32]; 1.5 g of Laponite (L1), MCM-41 (M1) or FSM-16 (F1), dried overnight at 120 °C under vacuum, were refluxed for 24 h with 0.9 cm^3 (3.8 mmol) of APTES in 100 cm^3 in dry toluene, under nitrogen atmosphere. After cooling the solid materials were filtered, Soxhlet extracted with toluene for 24 h and then dried at 120 °C, under vacuum, overnight. The functionalized materials were designated as L2 (for Laponite), M2 (for MCM-41) or F2 (for FSM-16).

Activation of APTES functionalized Laponite, MCM-41 and FSM-16: 1.0 g of L2 and M2 was refluxed for 4 h with 1.25 cm^3 (3.86 mmol) of a solution 21% in sodium ethoxide in ethanol. In the case of F2, 0.75 g of the material were refluxed for 24 h in 50 cm^3 of ethanol with 0.61 cm^3

of a solution 21% in sodium ethoxide (NaEtO). After filtering the solid materials they were Soxhlet extracted with ethanol for 24 h and then dried at 120 °C, under vacuum, overnight. It should be noticed that, because the APTES molecules are hydrolytically unstable, its p*K*a value cannot be evaluated directly and is normally approached by the value of the propylamine which is 10.6 [48, 49]. Considering the p*K*a of the ethanol as 15.9 [50] it can be found that the deprotonation of APTES by ethoxide is highly favored. The functionalized materials were designated as L4 (for Laponite), M4 (for MCM-41) or F4 (for FSM-16).

2.2.2 *Immobilisation of CAT 2*

Preparation of CAT 2: the complex (*R*,*R*)-[Mn(3,5-dtBut-salhd)Cl] (CAT 1, 0.05 g, 80 mmol) was dissolved in 50 cm^3 of acetonitrile, and to this solution 0.02 g (95 mmol) of $AgClO_4$ were added. The solution was stirred for 4 h at room temperature. After filtration of silver chloride and solvent removal a reddish brown complex (*R*,*R*)-[Mn(3,5-dtButsalhd)]ClO_4 (CAT 2) was obtained.

CAT 2 anchoring onto functionalized materials: a solution of CAT 2 (80 mg; 114 μmol) in 100 cm^3 of dichloromethane was refluxed for 4 h, and then left stirring overnight, with 1.0 g of L2, M2, L4 or M4. In the case of F2 and F4, a solution of complex CAT 2 (50 mg or 72 μmol for F2 and 40 mg or 57 μmol for F4) in 100 cm^3 of dichloromethane was refluxed for 12 h with 0.75 g of F2 and 0.50 g of F4. After cooling the solid materials were filtered, Soxhlet extracted with dichloromethane for 24 h and then dried at 120 °C, under vacuum, overnight to get the immobilized catalysts. The materials were designated as L3, M3, F3 (derived from L2, M2, F2) or L5, M5, F5 (derived from L4, M4, F4), respectively (where L, M and F, refers to the Laponite, MCM-41, and FSM-16 based materials, respectively), as shown in Scheme 1.

2.3 Characterization Methods

Nitrogen contents were obtained by elemental analysis at 'Laboratório de Análises', IST, Lisboa (Portugal). The bulk Mn content was determined by atomic absorption spectroscopy (AAS) in a Pye Unicam SP9 spectrometer. Typically one sample of 20 mg of solid, previously dried at 100 °C, was mixed with 2 cm^3 of aqua regia and 3 cm^3 of HF for 2 h at 120 °C, in a stainless steel autoclave equipped with a polyethylene-covered beaker (ILC B240). After reaching room temperature the solution was mixed with about 2 g of boric acid and finally adjusted to a known volume with deionized water.

Nitrogen adsorption isotherms at -196 °C were measured in an automatic apparatus (Asap 2010; Micromeritics). Before the adsorption experiments the samples were outgassed under vacuum during 2.5 h at 150 °C. Microporous volumes were estimated from the *t*-method [51] and mesoporous volumes from the amounts adsorbed at high relative pressures ($p/p^0 \sim 0.97$), and specific surface areas were obtained by the BET method [51]. Pore size distributions of the parent materials where obtained by the Non Linear Density Functional Theory [52, 53], see Supporting Information, SI1.

X-ray photoelectron spectroscopy was performed at "Centro de Materiais da Universidade do Porto" (Portugal), in a VG Scientific ESCALAB 200A spectrometer using a non-monochromatised Mg Kα radiation (1,253.6 eV). All the materials were compressed into pellets prior to the XPS studies. In order to correct possible deviations caused by electric charge of the samples, the C 1s line at 285.0 eV was taken as internal standard. The elemental contents of the various samples were calculated from the areas of the relevant bands in the high resolution XPS spectra.

2.4 Catalytic Experiments

The catalytic activity of the FSM-16 based materials in the asymmetric epoxidation of styrene, α-methylstyrene (α-Me-styrene) and 6-cyano-2,2-dimethylchromene (6-CN-chromene) was evaluated at 0 °C at atmospheric pressure in batch regimen, under constant stirring, using a mixture of *m*-chloroperoxybenzoic acid (*m*-CPBA) as oxidant and *N*-methylmorpholine (NMO) as co-oxidant. In the experiments 0.2 mmol of alkene, 0.2 mmol of chlorobenzene (internal standard), 90 mg of catalyst, 0.4 mmol of *m*-CPBA and 1.0 mmol of NMO in 5.00 cm^3 of dichloromethane were used. After 4 h of reaction the product analysis was made by GC-FID analysis using the internal standard method. After each cycle of utilization the catalyst was washed several times under refluxing condition with dichloromethane to remove occluded reactants and products. After drying the recovered catalyst at 100 °C in an oven, overnight, it was reused under identical condition.

The analysis of the products obtained after the catalytic experiments was done by GC-FID (using the internal standard method) on a Varian CP-3380 gas chromatograph equipped with a fused silica Varian Chrompack capillary column CP-Sil 8 CB Low Bleed/MS (30 m × 0.25 mm id; 0.25 μm film thickness), using helium as carrier gas. The enantiomeric excesses (%ee) of the epoxides were determined using the same chromatograph but using a fused silica Varian Chrompack capillary column CP-Chiralsil-Dex CB (25 m × 0.25 mm d.i. × 0.25 μm film thickness). Conditions used: 60 °C (3 min), 5 °C min^{-1}, 170 °C (2 min), 20 °C min^{-1}, 200 °C (10 min); injector temperature, 200 °C; detector temperature, 300 °C. The reaction

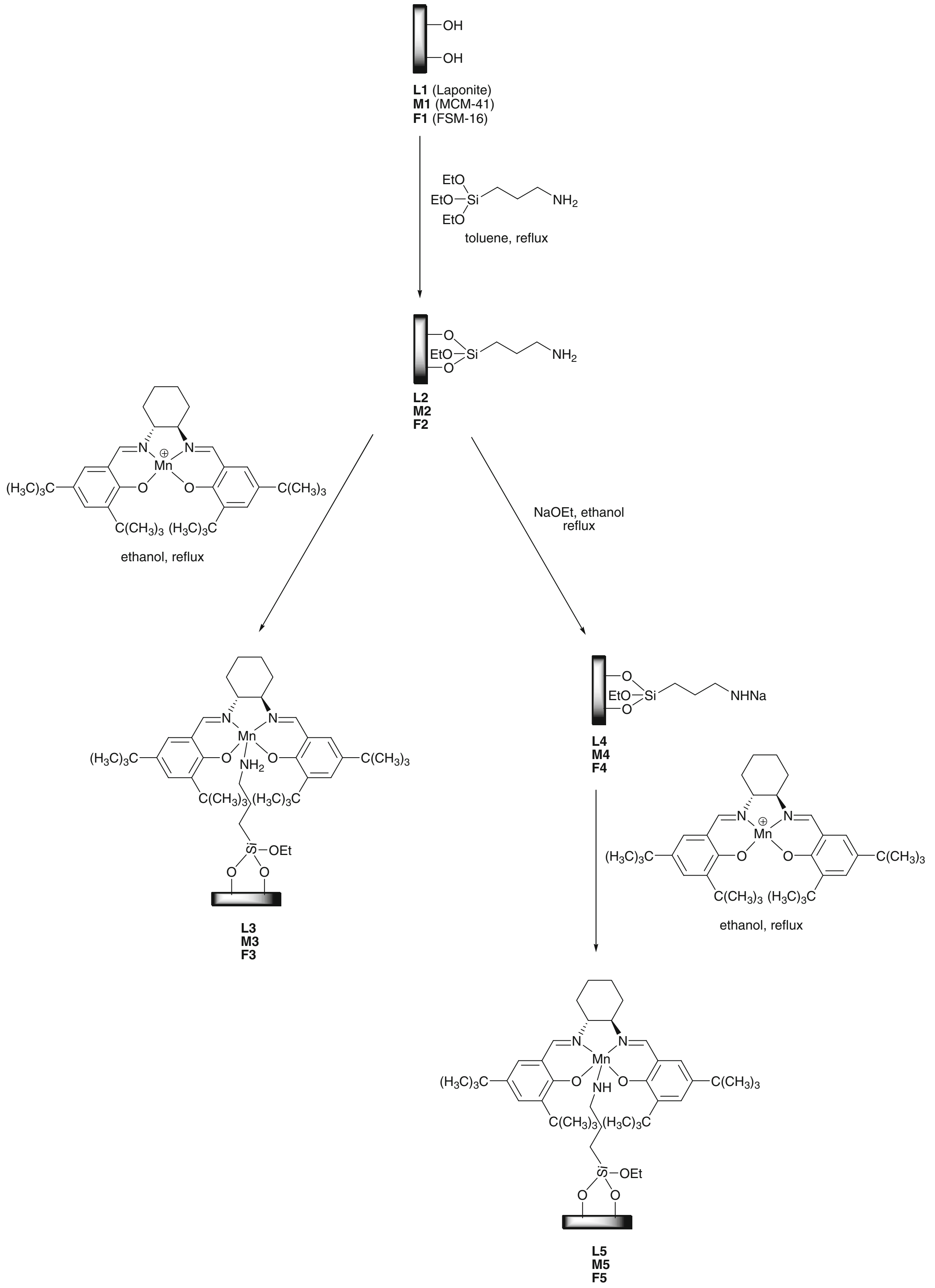

Scheme 1 Immobilization of CAT 2 onto amine-functionalized Laponite, MCM-41 and FSM-16

Table 1 Nitrogen and manganese contents determined from elemental analysis and XPS and textural properties of the Laponite, MCM-41 and FSM-16 base materials

Materials	N (mmol g^{-1})		Mn (μmol g^{-1})		Textural properties[d]		
	EA[a]	XPS[b]	AAS[c]	XPS[b]	A_{BET} (m^2/g)	V_{micro} (cm^3/g)	V_{meso} (cm^3/g)
L1	–	–	–	–	378	0.03	0.25
L2	1.1	1.56	–	–	122	0	0.13
L3	1.3	1.56	7.5	70	48	0	0.06
L4	0.51	0.45	–	–	n.d.	n.d.	n.d.
L5	0.51	0.64	16.0	26	73	0.02	0.04
M1	–	–	–	–	1087	0	0.86
M2	1.8	1.20	–	–	734	0	0.39
M3	1.7	1.21	8.0	168	340	0	0.21
M4	1.5	1.38	–	–	20	–	–
M5	1.6	1.35	1.2	21	5	–	–
F1	–	–	–	–	1323	0	0.95
F2	1.9	1.57	–	–	739		0.41
F3	1.4	1.25	9.6	21	689		0.35
F4	1.8	1.15			208		0.04
F5	1.3	[c]	16	[c]	557		0.28

[a] *EA* nitrogen elemental analysis; [b] *N or Mn* amount per weight of sample calculated from XPS data in Table SI2 (Supporting Information): mmol N or Mn/weight of sample = at% N or Mn/[at% *C* × Ar(C) + at% N × Ar(N) + at% O × Ar(O) + at% Mg × Ar(Mg) + at% Si × Ar(Si) + at% Cl × Ar(Cl) + at% Mn × Ar(Mn) + at% Na × Ar(Na)]; [c] *AAS* atomic absorption spectroscopy; [d] From the nitrogen adsorption isotherms at −196 °C

parameters $\%C$ (alkene conversion), $\%S_{epoxide}$ (epoxide selectivity), TON, TOF and ee% were calculated using the following formula, where A stands for area of chromatographic peak: $\%C = \{[A(\text{alkene})/A(\text{chlorobenzene})]_{t=0\text{h}} - [A(\text{alkene})/A(\text{chlorobenzene})]_{t=x\text{h}}\} \times 100/[A(\text{alkene})/A(\text{chlorobenzene})]_{t=0\text{h}}$, $\%S_{epoxide} = A(\text{epoxide}) \times 100/[A(\text{epoxide}) + \sum A(\text{other reaction products})]$, $\text{TON} = \%C \times \%S_{epoxide} \times \text{mmol (alkene)}_{t=0\text{h}}/\text{mmol Mn}$, TOF = TON/reaction time and $\%\text{ee} = [A(\text{major enantiomer}) - A(\text{minor enantiomer})] \times 100/[A(\text{major enantiomer}) + A(\text{minor enantiomer})]$.

3 Results and Discussion

The Mn(III) *salen* complex, CAT 2, was immobilized into two *N*-functionalized materials as summarized in Scheme 1: (1) directly anchored into APTES-functionalized Laponite, MCM-41 and FSM-16 (L2, M2 and F2) leading to materials L3, M3 and F3, respectively; and (2) anchored, after activation of the APTES-functionalized materials with NaOEt (L4, M4 and F4) originating materials denoted as L5, M5 and F5. These Mn(III) *salen*-based materials have been prepared and characterised by us previously [45, 46] and thus only the results from their characterisation that are relevant to the catalytic experiments will be discussed.

3.1 Modification of Laponite, MCM-41 and FSM-16 Surface

The specific surface areas (A_{BET}), microporous and mesoporous volumes for the different materials, obtained from the nitrogen desorption isotherms at −196 °C are given in Table 1.

The materials, Laponite, MCM-41 and FSM-16, can be divided into two groups of mesoporous materials possessing different textural properties: the external area material, Laponite, and the mainly internal area materials, MCM-41 and FSM-16. Their surface area (A_{BET}) and mesopore volume (V_{meso}) increase in the following order: Laponite (L1) $\ll$ MCM-41 (M1) < FSM-16 (F1), Table 1. Laponite possesses a smaller superficial area and mesopore volume, from the aggregation of the single crystals, than MCM-41 and FSM-16 which mesopore volume is mainly due to the internal channels (SI1, Supporting Information).

Evidence for APTES anchoring onto Laponite, MCM-41 and FSM-16 materials is given by nitrogen elemental analysis (EA) and nitrogen surface contents (XPS), Tables 1 and SI2 in Supporting Information: raw XPS data of the Laponite, MCM-41 and FSM-16 based materials. The two N contents increase in the order, Laponite (L2) $\ll$ MCM-41 (M2) < FSM-16 (F2), that correlate well with the materials surface area (A_{BET}) and mesopore

Table 2 Asymmetric epoxidation of alkenes at 0 °C using CAT 2 free or immobilised onto Laponite, MCM-41 and FSM-16[a]

Entry	Catalyst	Substrate	*t* (h)	*C*%[b]	ee%[c]	S_{epoxide}%[d]	TON[e]	TOF (h^{-1})[f]
1	CAT1	Styrene	1	73	44	91	151	151
2	CAT2		1	59	38	87	135	135
3	L3(1st)		4	32	26	86	135	34
4	L3 (2nd)		4	12	34	83	26	7
5	L3 (3rd)		4	4	15	49	5	1
6	M3 (1st)		4	12	9	39	12	3
7	M3 (2nd)		1	8	6	38	8	2
8	F3 (1st)		4	20	31	92	43	11
9	F3 (2nd)		4	8	5	77	12	3
10	L5(1st)		4	18	30	93	43	11
11	L5 (2nd)		4	7	4	27	2	0.5
12	F5 (1st)		4	40	38	90	50	12
13	F5 (2nd)		4	6	1	49	4	1
14	CAT1	α-Me-Styrene	1	97	48	91	185	185
15	CAT2		1	56	34	78	110	110
16	L3 (1st)		4	59	44	84	129	32
17	L3 (2nd)		4	19	28	72	37	9
18	L3 (3rd)		4	7	5	71	14	4
19	M3 (1st)		4	21	7	81	40	10
20	M3 (2nd)		4	12	6	65	19	5
21	F3 (1st)		4	24	33	92	49	12
22	F3 (2nd)		4	24	4	92	48	12
23	L5(1st)		4	44	31	87	50	12
24	L5 (2nd)		4	8	6	84	8	2
25	F5 (1st)		4	34	36	93	44	11
26	F5 (2nd)		4	10	6	100	14	3
27	CAT1	6-CN-Chromene	2	36	72	98	72	36
28	CAT2		2	33	67	94	71	35
29	L3 (1st)		4	22	64	96	53	13
30	L3 (2nd)		4	10	49	90	22	6
31	L3 (3rd)		4	7	23	48	8	2
32	M3 (1st)		4	14	26	100	34	8
33	M3 (2nd)		4	8	7	100	19	5
34	F3 (1st)		4	9	55	100	18	4
35	F3 (2nd)		4	14	11	80	23	6
36	F5 (1st)		4	15	62	84	17	4
37	F5 (2nd)		4	14	1	100	18	5

[a] Reactions were carried out with 90 mg of heterogeneous catalyst, in dichloromethane at 0 °C; alkene: *m*-CPBA:NMO = 1:2:5; reaction time = 4 h

[b] Relative to alkene

[c] Determined by chiral GC-FID

[d] Determined by GC-FID, against internal standard (chlorobenzene)

[e] Total TON based on the alkene conversion

[f] TOF = TON/reaction time

volume (V_{meso}). Moreover, for L2 the nitrogen content obtained by AE is lower than that by XPS, whereas for M2 and F2 the opposite is observed (Tables 1; SI2). These results show that APTES is mainly located externally in Laponite, at the edges of the Laponite single crystals, whereas in MCM-41 and FSM-16 is mainly grafted in the material pore walls.

Activation of APTES-functionalized materials by NaOEt increase the material sodium surface content, but a decrease of surface nitrogen content was also observed (L4, M4 and F4 in Table SI2), probably due to leaching of some grafted APTES molecules during the activation procedure. This treatment also creates, for M4 and F4, a new porosity in a region for values higher than 4 nm, [45, 46] inexistence for parent MCM-41 and FSM-16. Furthermore, for M4, there is also a significant decrease in the A_{BET} values, a consequence of the mesoporous structure collapse, confirmed by XRD data, as described elsewhere [45, 46].

3.2 Mn(III) *Salen* Anchoring

The Mn loading in the APTES-functionalized materials increases in the order L3 < M3 < F3, which correlate well with A_{BET}, V_{meso} and N content of the corresponding materials (Table 1), whereas for the activated APTES-functionalized materials the Mn loading is M5 $\ll$ L5 = F5. While for L5 and F5 the Mn loading is double of that of L3 and F3, a big decrease in Mn content is observed for M5 compared to M3. This may be attributed to some collapse of the MCM-41 porous structure upon NaOEt activation (Table 1), decreasing its capacity to anchor the Mn(III) *salen* complex (CAT 2).

In the APTES functionalized materials, CAT 2 is immobilized through metal center coordination onto the surface amine groups as described elsewhere [4–12, 45, 46]; for L5, M5 and F5 materials the observed decrease in surface Na surface contents (Table SI2) upon complex immobilization, indirectly prove that CAT 2 is immobilized through metal center coordination onto the new anionic nitrogen species, by exchanging the sodium cation.

Upon complex anchoring the textural properties of the materials change significantly, Table 1: for F3/M3 and F5 there are decreases (in relation to their parent materials) in A_{BET} and V_{meso} that suggest that CAT 2 is anchored inside the pores, but for L3 and L5 samples, the surface area decrease (in relation to L2), is due to the fact that the complex can promote a different arrangement of the crystallites.

3.3 Catalysis Experiments

3.3.1 First Catalytic Cycle

With the exception of M5, which possesses a very low Mn loading, the other materials with immobilized CAT 2 (L3, M3, F3, L5 and F5) were tested as heterogeneous catalysts in the asymmetric epoxidation of three alkenes (styrene, α-methyl-styrene and 6-cyano-2,2-dimethylchromene) at 0 °C, using *m*-chloroperoxybenzoic acid (*m*-CPBA) as oxygen source and 4-methylmorpholine *N*-oxide (NMO) as co-oxidant. The results are compiled in Table 2 and Fig. SI3, Supporting Information, together with the results obtained in homogeneous phase with CAT 2 and CAT 1, under the same experimental conditions.

It is noteworthy that substitution of the chloride anion in the *Jacobsen* catalyst (CAT1) by the non-coordinating perchlorate anion (CAT2) results in a moderate general decrease in the catalytic reaction parameters, for example: styrene, entry 1 versus 2: *C*% from 73 to 59 and ee% from 44 to 38; α-Me styrene, entry 14 versus 15: *C*% from 97 to 56 and ee% from 48 to 34; whereas a very little decrease for the 6-CN-chromene (entry 27 vs. 28: *C*% from 36 to 33; ee% from 72 to 67) was observed. These results show that the axial coordination position of the *Jacobsen* catalyst is extremely important in the asymmetric epoxidation outcome.

All the heterogeneous catalysts tested, L3, M3, F3, L5 and F5, were active, enantioselective and generally highly chemoselective in the asymmetric epoxidation of the three alkenes, whereas their corresponding precursors materials showed negligible activity under the same experimental conditions. For all the catalysts studied the order of epoxide ee% and alkene epoxide selectivity ($S_{epoxide}$%) are generally (Table 2; Fig. SI3): 6-CN-chromene (64–26 and 100–84%) > α-Me-styrene (44–7 and 93–81%) > styrene (38–9 and 93–39%). The alkene conversion% is generally: α-Me-styrene (59–21%) > styrene (40–12%) > 6-CN-chromene (22–9%). The order for the TON and TOF are: styrene (135–12 and 34–3 h^{-1}) ≥ α-Me-styrene (129–40 and 32–10 h^{-1}) > 6-CN-chromene (53–17 and 13–4 h^{-1}).

With exception of M3 catalyst, the enantioselectivity and epoxide selectivitiy of the heterogeneous catalysts are comparable or higher than those obtained with CAT 2 in homogeneous phase. In fact, an increase in activity and enantioselectivity was observed for the epoxidation of α-Me-styrene with L3 catalyst (entry 15 vs. 16: *C*% from 56 to 59; ee% from 36 to 44 and TON from 110 to 129). F5 catalyst also presents in the epoxidation of α-Me styrene higher ee% than CAT2 (entry 15 vs. 25: ee% from 34 to 36) and in the epoxidation of styrene similar ee% (entry 2 vs. 12: ee% = 38).

There are some reports on the enhancement of the enantioselectivity of the *Jacobsen* catalyst upon metal center axial anchoring to the mesopore surface of functionalised MCM-41. Li et al. immobilised the *Jacobsen* catalyst onto MCM-41 via axial metal center coordination of oxygen either from a phenoxy group [20] or from phenyl sulfonic group [21] grafted on the surface of MCM-41 which lead to markedly higher ee% (72–78) for epoxidation of α-Me-styrene using NaOCl as oxygen at 0 °C in CH_2Cl_2 after 24 h of reaction, as compared to its homogeneous analog (ee%: 55–56%), which was mainly attributed to the unique spatial environment constituted by the axial bulky group and the mesopores of the MCM-41 support [20–23]. Enhancement of the enantioselectivity was also reported by

Kim and Shin [19] and Zhou et al. [30], respectively. Kim and Shin [19] reported that, for the asymmetric epoxidation of α-Me-styrene, the ee% increased from 51 to 59% after immobilisation of Mn(III) *salen* on the siliceous MCM-41 by a multi-step grafting through the ligand. For the enantioselective epoxidation of *β*-methylstyrene, the ee% increased from 54 to 73% after immobilization of Cr(III) *salen* through coordination of the metal center to NH_2 surface grafted groups [30]. These results clearly indicate that in addition to the support material, the nature of anchoring group (axial ligand), and also how it is anchored with the metal, plays a significant role in the activity and enantioselectivity of the immobilized catalyst.

Nevertheless, the heterogeneous reactions were slower than in homogeneous phase, which is obviously due to the slow diffusion of the reactant and the oxidant to the active sites in the multiphase reaction system, and therefore CAT 2 immobilized onto all the functionalized materials presents generally lower catalytic activity than the free CAT 2, with the exception discussed above.

The most efficient and active heterogeneous catalyst for all the alkenes tested was L3 yielding the highest TON and TOF of all the heterogeneous catalysts tested (Table 2). This can be explained by two issues: (1) low Mn content, proving that the heterogeneous epoxidation of alkenes by Mn(III) *salen* complexes works efficiently with very low Mn molar percentages in the reaction mixture (Table 1) and that higher Mn loading in a catalyst does not necessarily lead to a better catalyst performance, (2) lower diffusion limitations since in Laponite the anchoring of CAT 2 occurs on the external surface, making it easier for the reactant to interact with the catalyst active site. These may explain why L3 catalyst acted as one of the most enantioselective heterogeneous catalysts in the asymmetric epoxidation of α-Me styrene and 6-CN-chromene, presenting lower steric hindrances during the course of the epoxidation with the biggest alkenes, in comparison with the MCM-41 and FSM-16 materials. In these latter materials, the reactive –OH groups, and therefore APTES, are mainly confined to the internal surface of the hexagonal channels. Consequently CAT 2 is mainly immobilized onto the inside pore channel and hence are relatively unapproachable for the substrates. Nevertheless, F5 and F3 acted as better catalysts in the asymmetric epoxidation of styrene than L3, which may be attributed to a favorable geometry of the pores.

Furthermore, F5 material gives higher enantioselectivity and alkene conversion for all the alkenes than F3, indicating improved performance of the CAT 2 when anchored onto the activated APTES-functionalized FSM-16. For Laponite only in the asymmetric epoxidation of styrene an improved ee% is observed for L5 compared to L3. It is also known that the addition of strong Lewis bases to Mn(III) *salen* complexes results in improved enantioselectivity in their asymmetric epoxidation of alkenes [1–3, 20–26]. Therefore, the increase in enantioselectivity upon NaOEt treatment may be attributed to the increase of basicity of the surface nitrogen groups which coordinate to the Mn center of CAT 2.

Table 3 Bulk Mn content and N_2 adsorption values for the Laponite-based material L3 after catalysis (2 cycles)

Substrate	Mn (μmolg^{-1})[a]	A_{BET} (m^2/g)[b]
Before	7.5	48
Styrene	5.0	11
α-Me-Styrene	8.7	19
6-CN-Chromene	4.8	3

[a] AAS; [b] N_2 adsorption at −196 °C

It is worth mentioning that the catalysts prepared with FSM-16 material (F3 and F5) were generally more active, chemoselective and enantioselective than the catalyst prepared with MCM-41 material (M3), showing the superiority of the FSM-16 as a mesoporous support for Mn(III) *salen* catalysts than the often used MCM-41.

3.3.2 Recycling Experiments

The reutilization of all the heterogeneous catalysts in a further catalytic cycle leads a gradual decrease of epoxide enantioselectivity and selectivity and, generally, of alkene conversion (Table 1), suggesting deactivation or leaching of catalyst by oxidative degradation of the anchored complex under the experimental conditions used.

Analyzing the properties of Laponite-based material L3 after catalysis, Table 3, we can infer that the leaching of the metal complex from the support under catalytic conditions may not be considered the sole reason for the reduction of catalytic activity. For instance, the Mn contents of the Laponite based materials after epoxidation of styrene and 6-CN-Chromene decrease 32 and 35%, respectively, whereas the *C* and ee% values, for styrene, drop off 88 and 45% and for 6-CN-Chromene, reduce 70 and 65%, respectively. Secondly, the A_{BET} values for these materials after catalysis show that there is almost no further space available for the N_2 adsorption. These can be due to side products, as well as residues from the oxygen sources, that adsorb strongly and irreversibly at the surface of the materials under the conditions used, even after purification of the reused catalysts. This occurrence leads to blocking of the catalyst's pore mouth, inducing their deactivation, and occurs concomitantly to Mn(III) complex leaching.

4 Conclusions

In this work we used two types of APTES modified supports for the immobilization of a chiral Mn(III) *salen* complex, CAT 2: laponite, which has a relatively high surface area (378 m^2 g^{-1}), but where the surface area is essential external and it originates from the inter-particle aggregation of this finely divided material, and two regular mesoporous materials (MCM-41 and FSM-16), in which the surface area come from the internal porosity, that is, from the well defined pores.

The comparison between the efficiency of all heterogeneous catalysts for the enantioselective epoxidation of several alkenes showed essential two main conclusions. Firstly, finely divided materials with high surface areas and appropriate surface groups, are also an option that deserve wider studies considering its application as supports of enantioselective catalysts (cf. sample L3 in Scheme 1). Secondly, in the case of mesoporous supports in which the surface area comes from the internal porosity the chemical stability of the support is mandatory both, in the reaction conditions as well as in the intermediate steps of surface modification of the support. In the methodologies used in this work, FSM-16 based materials showed better results than the MCM-41 type materials, confirming what has been published in literature relating the higher stability of FSM-16 compared with MCM-41.

Acknowledgments This work was funded by FCT Fundação para a Ciência e a Tecnologia (FCT) and FEDER, through the project ref. POCI/CTM/56192/2004. PD thanks FCT for a Post-Doctoral fellowship. Thanks are due to Dr. Shinji Inagaki, from Toyota Central R&D Labs for the FSM-16 sample.

References

1. McGarrigle EM, Gilheany DG (2005) Chem Rev 105:1563
2. Jacobsen EN, Wu MH (1999) In: Pfaltz A, Jacobsen EN, Yamamoto H (eds) Comprehensive asymmetric catalysis. Springer, Berlin, p 649
3. Katsuki T (1995) Coord Chem Rev 140:189
4. Li C (2004) Catal Rev 46:419
5. McMorn P, Hutchings GJ (2004) Chem Soc Rev 33:108
6. Fan QH, Li YM, Chan ASC (2002) Chem Rev 102:3385
7. Smith K, Liu CH (2002) Chem Commun 886
8. Reger TS, Janda KD (2000) J Am Chem Soc 122:6929
9. Song CE, Roh EJ, Yu BM, Chi DY, Kim SC, Lee KJ (2000) Chem Commun 615
10. Canali L, Cowan F, Deleuze H, Gibson CL, Sherrington DC (2000) J Chem Soc Perkin Trans 1:2055
11. Angelino MD, Laibinis PE (1999) J Polym Sci Polym Chem 37:3888
12. Minutolo F, Pini D, Petri A, Salvadori P (1996) Tetrahedron Asymmetry 7:2293
13. Sabater MJ, Corma A, Domenech A, Fornés V, Garcia H (1997) Chem Commun 1285
14. Ogunwumi SB, Bein T (1997) Chem Commun 901
15. Heinrichs C, Hölderich WF (1999) Catal Lett 58:75
16. Gbery G, Zsigmond A, Balkus KJ Jr (2001) Catal Lett 74:77
17. Bigi F, Moroni L, Maggi R, Sartori G (2002) Chem Commun 716
18. Kim G-J, Kim S-H (1999) Catal Lett 57:139
19. Kim G-J, Shin J-H (1999) Tetrahedron Lett 40:6827
20. Xiang S, Zhang Y, Xin Q, Li C (2002) Chem Commun 2696
21. Zhang H, Xiang S, Li C (2005) Chem Commun 1209
22. Zhang H, Xiang S, Xiao J, Li C (2005) J Mol Catal A: Chem 238:175
23. Zhang H, Xiang S, Li C (2006) J Catal 238:369
24. Kureshy RI, Ahmad I, Khan NH, Abdi SHR, Singh S, Pandia PH, Jasra RV (2005) J Catal 235:28
25. Cardoso B, Pires J, Carvalho AP, Biernacka IK, Silva AR, de Castro B, Freire C (2005) Microporous Mesoporous Mater 86:295
26. Biernacka IK, Silva AR, Carvalho AP, Pires J, Freire C (2007) J Mol Catal A: Chem 278:82
27. Silva AR, Wilson K, Clark JH, Freire C (2006) Microporous Mesoporous Mater 91:128
28. Jones MD, Raja R, Thomas JM, Johnson BFG, Lewis DW, Rouzaud J, Harris KDM (2003) Angew Chem Int Ed 42:4326
29. Raja R, Thomas JM (2002) J Mol Catal A: Chem 181:3
30. Zhou XG, Yu XQ, Huang JS, Li SG, Li LS, Che CM (1999) Chem Commun 1789
31. Baleizão C, Gigante B, Sabater MJ, Garcia H, Corma A (2002) Appl Catal A: Gen 288:179
32. Dioos BML, Geurts WA, Jacobs PA (2004) Catal Lett 97:125
33. Serrano DP, Aguado J, Garcia RA, Vargas C (2005) In: Čejka J, Žilková N, Nachtigal P (eds) Molecular sieves: from basic research to industrial applications, studies in surface science and catalysis, vol 158B. Elsevier, Amsterdam, p 1493
34. Kureshy RI, Khan NH, Abdi SHR, Ahmad I, Singh S, Jasra RV (2004) J Catal 221:234
35. Kureshy RI, Khan NH, Abdi SHR, Ahmad I, Singh S, Jasra RV (2003) Catal Lett 91:207
36. Fraile JM, Garcia JI, Massam J, Mayoral JA (1998) J Mol Catal A: Chem 136:47
37. Dixit PS, Srinivasan K (1988) Inorg Chem 27:4507
38. Wheeler PA, Wang J, Baker J, Mathias LJ (2005) Chem Mater 17:3012
39. Kuźniarska-Biernacka I, Silva AR, Carvalho AP, Pires J, Freire C (2005) Langmuir 21:10825
40. Inagaki S, Fukushima Y, Kuroda K (1993) J Chem Soc Chem Commun 680
41. Inagaki S, Koiwai A, Suzuki X, Fukushima Y, Kuroda K (1996) Bull Chem Soc Jpn 69:1449
42. Igarashi N, Koyano KK, Tanaka Y, Nakata S, Hashimoto K, Tasumi T (2003) Microporous Mesoporous Mater 59:43
43. Kresge CT, Leonowicz ME, Roth WJ, Vartuli JC, Beck JS (1992) Nature 359:710
44. Fenelonov VB, Romannikov VN, Derevyankin AY (1999) Microporous Mesoporous Mater 28:57
45. Das P, Silva AR, Carvalho AP, Pires J, Freire C submitted
46. Das P, Silva AR, Carvalho AP, Pires J, Freire C (2008) Colloids Surf A: Physicochem Eng Asp 329:190
47. Grün M, Unger KK, Matsumoto A, Tsutsumi K (1997) In: McEnaney B, Mays T, Rouquerol J, Rodríguez-Reinoso F, Sing K, Unger KK (eds) Characterisation of porous solids IV. The Royal Society of Chemistry, p 81
48. Benazilla M, Manne S, Laney DE, Lyubchenko YL, Hansma HG (1995) Langmuir 10:665
49. Tatsumi T (2005) Proceedings of 15th Saudi-Japan Joint Symposium. Dahram, Saudi Arabia
50. Handbook of chemistry and physics (1972) 53 edn. CRC Press, Boca Raton
51. Rouquerol F, Rouquerol J, Sing K (1999) Adsorption by powders & porous solids. Academic Press, New York
52. Olivier JP (1995) J Porous Mater 2:9
53. Olivier JP, Occelli ML (2001) J Phys Chem B 105:623